AD-A145 587 ELECTRONIC-TO-VIBRATIONAL ENERGY TRANSFER STUDIES OF SINGLET MOLECULAR OX.. (U) KANSAS STATE UNIV MANHATTAN J P SUNG ET AL. JUL 84 AWWL-TR-84-23 F29601-82-K-0088 1/1

UNCLASSIFIED F/G 20/8 NL

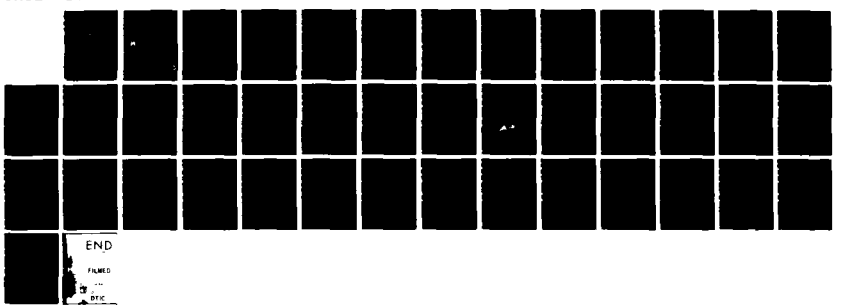

END

FILMED

DTIC

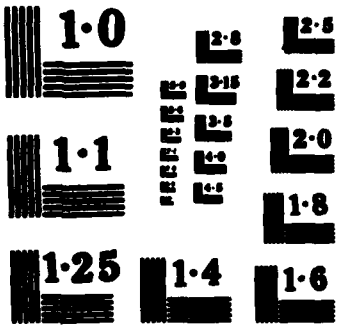
1·0
1·1
1·25
2·8
3·15
3·5
4·0
1·4
2·5
2·2
2·0
1·8
1·6

AFWL-TR-
84-23

ELECTRONIC-TO-VIBRATIONAL ENERGY TRANSFER STUDIES OF SINGLET MOLECULAR OXYGEN AND HYDROGEN HALIDES

Jageish P. Sung
Juheda Bachar
Donald W. Setser

Kansas State University
Manhattan, KS 66506

July 1984

Final Report

Approved for public release; distribution unlimited.

AIR FORCE WEAPONS LABORATORY
Air Force Systems Command
Kirtland Air Force Base, NM 87117

AFWL-TR-84-23

This final report was prepared by Kansas State University, Manhattan, Kansas under Contract F29601-82-K-0088, Job Order ILIR8209 with the Air Force Weapons Laboratory, Kirtland Air Force Base, New Mexico. Nicholas R. Pchelkin (ARDD) was the Laboratory Project Officer-in-Charge.

When Government drawings, specifications, or other data are used for any purpose other than in connection with a definitely Government-related procurement, the United States Government incurs no responsibility or any obligation whatsoever. The fact that the Government may have formulated or in any way supplied the said drawings, specifications, or other data, is not to be regarded by implication, or otherwise in any manner construed, as licensing the holder, or any other person or corporation; or as conveying any rights or permission to manufacture, use, or sell any patented invention that may in any way be related thereto.

This report has been authored by a contractor of the United States Government. Accordingly, the United States Government retains a nonexclusive, royalty-free license to publish or reproduce the material contained herein, or allow others to do so, for the United States Government purposes.

This report has been reviewed by the Public Affairs Office and is releasable to the National Technical Information Services (NTIS). At NTIS, it will be available to the general public, including foreign nations.

If your address has changed, if you wish to be removed from our mailing list, or if your organization no longer employs the addressee, please notify AFWL/ARDD, Kirtland AFB, NM 87117 to help us maintain a current mailing list.

This technical report has been reviewed and is approved for publication.

Nicholas R Pchelkin

NICHOLAS R. PCHELKIN
Project Officer

FOR THE COMMANDER

Orven F Swenson

ORVEN F. SWENSON
Maj, USAF
Chief, Short Wavelength Laser Branch

Winston K Pendleton

WINSTON K. PENDLETON
Col, USAF
Ch, Laser Science & Tech Office

DO NOT RETURN COPIES OF THIS REPORT UNLESS CONTRACTUAL OBLIGATIONS OR NOTICE ON A SPECIFIC DOCUMENT REQUIRES THAT IT BE RETURNED.

UNCLASSIFIED

SECURITY CLASSIFICATION OF THIS PAGE

REPORT DOCUMENTATION PAGE

1a. REPORT SECURITY CLASSIFICATION: Unclassified	1b. RESTRICTIVE MARKINGS
2a. SECURITY CLASSIFICATION AUTHORITY	3. DISTRIBUTION/AVAILABILITY OF REPORT: Approved for public release; distribution unlimited.
2b. DECLASSIFICATION/DOWNGRADING SCHEDULE	
4. PERFORMING ORGANIZATION REPORT NUMBER(S)	5. MONITORING ORGANIZATION REPORT NUMBER(S): AFWL-TR-84-23
6a. NAME OF PERFORMING ORGANIZATION: Kansas State University; 6b. OFFICE SYMBOL (If applicable)	7a. NAME OF MONITORING ORGANIZATION: Air Force Weapons Laboratory
6c. ADDRESS (City, State and ZIP Code): Manhattan, KS 66506	7b. ADDRESS (City, State and ZIP Code): Kirtland AFB NM 87117
8a. NAME OF FUNDING/SPONSORING ORGANIZATION; 8b. OFFICE SYMBOL (If applicable)	9. PROCUREMENT INSTRUMENT IDENTIFICATION NUMBER: F29601-82-K-0088
8c. ADDRESS (City, State and ZIP Code)	10. SOURCE OF FUNDING NOS.

PROGRAM ELEMENT NO.	PROJECT NO.	TASK NO.	WORK UNIT NO.
61101F	ILIR	82	09

11. TITLE (Include Security Classification): ELECTRONIC-TO-VIBRATIONAL ENERGY TRANSFER STUDIES OF SINGLET OXYGEN AND HYDROGEN HALIDES (U)

12. PERSONAL AUTHOR(S): Sung, Jagdish P., Bachar, Juheda, Setser, Donald W.

13a. TYPE OF REPORT	13b. TIME COVERED	14. DATE OF REPORT (Yr., Mo., Day)	15. PAGE COUNT
Final Report	FROM Aug 82 TO Nov 83	1984, July	41

16. SUPPLEMENTARY NOTATION

17. COSATI CODES			18. SUBJECT TERMS (Continue on reverse if necessary and identify by block number)
FIELD	GROUP	SUB. GR.	Singlet oxygen, Electronic-to-vibrational Energy Transfer, Infrared Emission HF, HCl, HBr, HCN
07	04		
20	05		

19. ABSTRACT (Continue on reverse if necessary and identify by block number)

Electronic-to-vibrational (E-V) energy transfer reaction of $O_2(b^1\Sigma^+)$ and $O_2(a^1\Delta g)$ were studies by simultaneously observing the decay of the $O_2(a)$ and $O_2(b)$ concentrations and the growth of the infrared emission intensity from the product states. The experiments were done in a flowing afterglow apparatus. Infrared (IR) emission measurements were made for $O_2(b)$ reacting with HF, HCl, HBr and HCN, and for $O_2(a)$ reacting with HF. Quenching data were taken for these molecules and for several other small molecules for which E-V energy transfer is the quenching mechanism.

20. DISTRIBUTION/AVAILABILITY OF ABSTRACT	21. ABSTRACT SECURITY CLASSIFICATION	
UNCLASSIFIED/UNLIMITED ☒ SAME AS RPT. ☐ DTIC USERS ☐	Unclassified	
22a. NAME OF RESPONSIBLE INDIVIDUAL: Nicholas R. Pchelkin	22b. TELEPHONE NUMBER (Include Area Code): (505) 844-1871	22c. OFFICE SYMBOL: AFWL/ARDO

DD FORM 1473, 83 APR EDITION OF 1 JAN 73 IS OBSOLETE.

UNCLASSIFIED

SECURITY CLASSIFICATION OF THIS PAGE

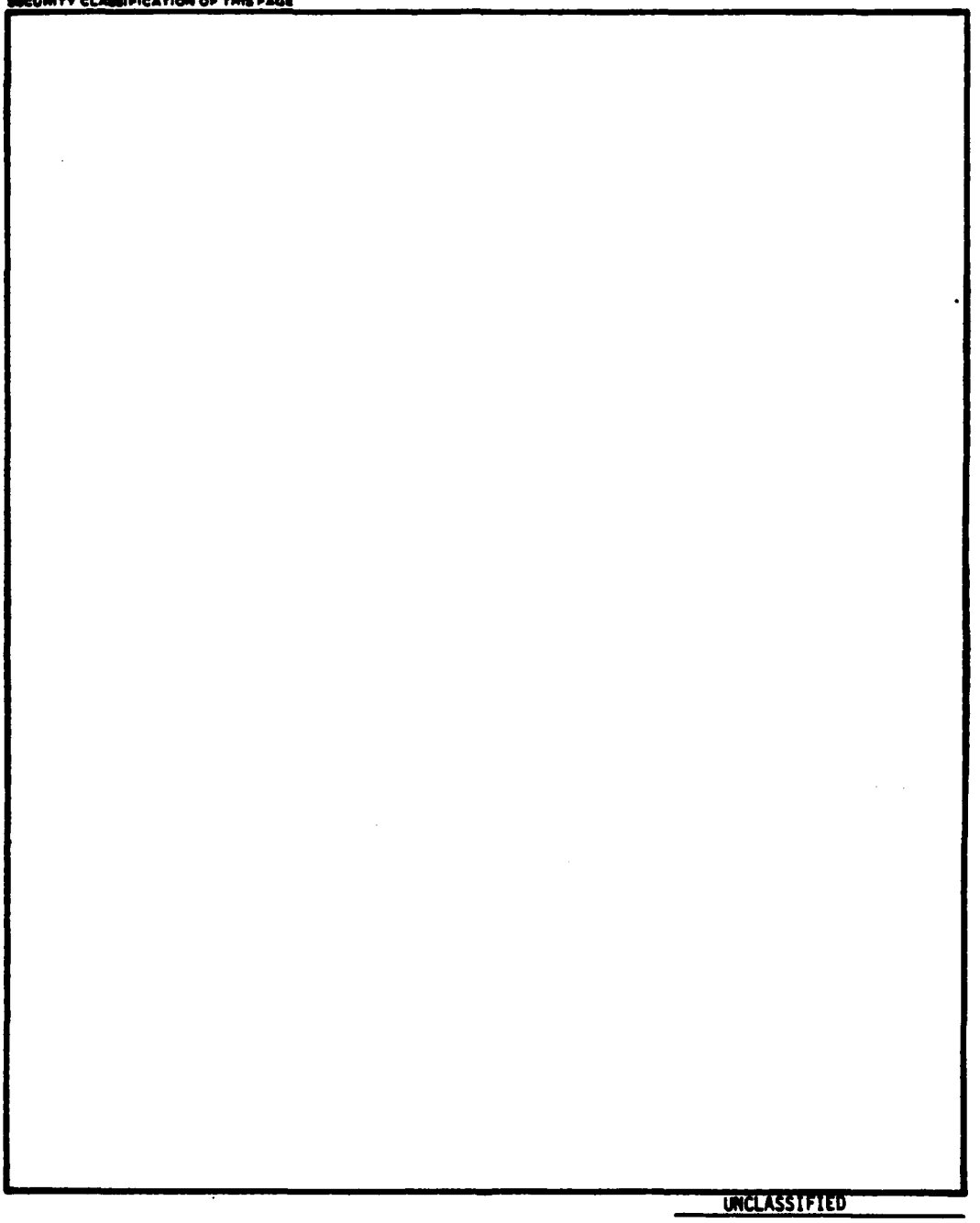

CONTENTS

FIGURES

TABLES

I. INTRODUCTION

The first two excited states of molecular oxygen, $O_2(a^1\Delta_g)$ - 0.997 eV and $O_2(b^1\Sigma_g^+)$ - 1.627 eV, with radiative lifetime of 65 min and 12 sec, respectively, are interesting candidates for electronic-to-vibrational (E-V) energy studies because high concentrations can be conveniently generated by chemical means (Ref. 1). The iodine-oxygen chemical laser (Ref. 2) is evidence for the possible utility of singlet oxygen, if a good E-V transfer system could be discovered. Interest in reactions of singlet O_2 was initially aroused in this laboratory by the accidental observation of infrared emission from HF, HCl and HBr during a study (Ref. 3) of the reaction of O atoms with HI. This interest was augmented by a collaboration with Professor Rosenwaks, Ben Gurion University, who was studying the O_2/I system (Ref. 4) and metal atom oxidation by singlet oxygen (Ref. 5). This report presents the study of E-V energy transfer from $O_2(a^1\Delta_g)$ and $O_2(b^1\Sigma_g^+)$ to hydrogen halides and HCN at the state-to-state level. The singlet oxygen was generated by either microwave discharge or chemical generator methods in a flow reactor. Since $O_2(b)$ is always present because of the bimolecular energy pooling reaction of $O_2(a)$, and since the rate of $O_2(b)$ reactions are faster than those of $O_2(a)$, it was necessary to isolate the quenching reactions of these two species in order to characterize the E-V transfer processes at the state-to-state level. The decay of both $O_2(a)$ and $O_2(b)$ concentrations were monitored simultaneously with the growth of the infrared emission of the products. The infrared emission was observed with

$$O_2(b^1\Sigma_g^+) + HX(X = F, Cl, Br, CN) \rightarrow O_2(a^1\Delta_g) + HX(v) \quad (a)$$
$$\rightarrow O_2(X^3\Sigma_g^-) + HX(v) \quad (b) \qquad (1)$$

$$O_2(a^1\Delta_g) + HX(X = F, Cl, Br, CN) \rightarrow O_2(X^3\Sigma_g^-) + HX(v) \qquad (2)$$

a Fourier transform spectrometer using standard techniques developed in the Kansas State University (KSU) laboratory (Refs. 3,6). The goal of measuring rate constants

and product distributions was achieved for reaction (1). However, for reaction (2), only the HF reaction could be studied at the state-to-state level because the quenching rates were so slow. In addition to the state-to-state studies of reactions (1) and (2), some work was done to measure the total quenching rate constants for $O_2(a)$ and $O_2(b)$ for several molecules other than the hydrogen halides. The quenching rate constants for $O_2(a^1\Delta_g)$ are small, and electronic-to-vibrational energy transfer is not a facile process. The singlet oxygen source in this experiment was usually a microwave discharge, although a chemical generator was available. The principal problem associated with use of a chemical generator in this work was the large, but uncertain, concentration of H_2O, which has large rate constants for vibrational relaxation of the product states from (1) and (2). After reviewing some of the more relevant published work, the KSU measurements are described.

Wayne's review article (Ref. 7) of 1969 summarized microwave discharge generation and the detection of singlet oxygen for studies in flow reactors. O'Brien and Myers (Ref. 8) showed that relaxation of a perturbed $O_2(b)$ steady-state could be used for the measurement of $O_2(b)$ quenching rate constants in a flow reactor. Becker and coworkers (Ref. 9) studied the quenching rate constants for both $O_2(b)$ and $O_2(a)$ using a stainless-steel sphere (2.2×10^5 litres) and measuring the decay of $O_2(b)$ and $O_2(a)$ concentrations with time for a particular concentration of reagent. The most comprehensive study of E-V transfer is that of Thomas and Thrush (Ref. 10), who measured the quenching of $O_2(a)$ and $O_2(b)$ and also the product infrared emission from a 10-liter integrating sphere. The spirit of that work closely resembles our own; however, the degree of vibrational relaxation is more easily monitored in a flow reactor than in an integrating sphere. Ogryzlo and Thrush[10d] observed vibrational excitation of H_2O and CO_2 from $O_2(b)$ reactions. Madronich, et al. (Ref. 11), reported E-V energy transfer from singlet oxygen to

HF, and suggested that the HF emission was mainly due to $O_2(a)$, rather than $O_2(b)$, because of the existence of the resonance match of HF(v=2) with $O_2(a)$ and because of the order dependence of the emission intensity on $[O_2(a)]$. However, the work was not definitive. Recently Borrell and coworkers (Ref. 12d) have measured quenching rate constants for $O_2(b)$ and $O_2(a)$ for several small molecules in a flow reactor at room temperature as part of a comprehensive program (Ref. 12) for studying the temperature dependence of the quenching of $O_2(b)$ and $O_2(a)$. Wayne and coworkers (Ref. 13) have recently shown that a flow reactor can be used for study of slow reactions and reported an upper limit for quenching of $O_2(a)$ by CO_2.

The quenching of $O_2(b)$ also can be studied in real time by using lasers (Refs. 14-16) to pump molecules from $O_2(X^3\Sigma_g^-)$ to $O_2(b^1\Sigma_g^+)$, photolysis of O_2 using a VUV H_2 laser (Ref. 17) ($\lambda\sim$160 nm) or photolysis of O_3. The last two methods depend upon excitation-transfer from $O(^1D)$ to $O_2(X)$ to give $O_2(b)$. The temperature dependence studies for the rate constant of $O_2(b)$ with HBr (Ref. 18) and HCl (Ref. 17) are of direct interest to the KSU work. The E-V transfer from $O_2(b)$ to CO_2 recently has been observed (Ref. 16) in real time by monitoring both reactants and products.

Generally the quenching of $O_2(b)$ and especially $O_2(a)$ by closed shell molecules is slow (Ref. 19). In contrast, the reactions with non-closed shell atoms, even those without suitable low energy acceptor electronic states, is appreciably faster; thus, the quenching (Refs. 20-22) rate constants for $O_2(a)$ by O, H, N are in the range of 10^{-14} cm^3 molec^{-1} s^{-1}. Of course, if low energy electronic states are available, the $O_2(a)$ and $O_2(b)$ quenching rate constants are much larger, as the well-known transfer between $O_2(a)$ and atomic iodine demonstrates (Refs. 2c-e). Another example is the reaction of $O_2(a)$ with Pb (Ref. 5), which gives PbO* and Pb*.

Winter, et al (Ref. 23), have studies the emission from SeO, SeS and Se_2 from the reaction of O_2 with SeO, SeS, and Se_2; and McDermott and Bernard (Ref. 24) observed SeO($B^3\Sigma^- - X^3\Sigma^-$) emission in the reaction of $O_2(a)$ with selenium

vapor. The excitation mechanism for SeO(b) was thought to depend on rapid excitation transfer between $O_2(a)$ and Se.

There have been various attempts to explain E-V transfer (Ref. 19) from $O_2(a)$ and $O_2(b)$. Kear and Abraham (Ref. 25) used a short range interaction model; but their rate constants are generally 2-3 orders of magnitude smaller than the experimental values. Braithwaite et al. (Ref. 26) developed a long-range multipole interaction model and calculated the quenching constants for $O_2(b)$ and $O_2(a)$ by diatomic molecules. Their calculated values are in better agreement with experimental data but some cases still differ by 2-3 orders of magnitude. Thomas and Thrush (Ref. 10c) applied a statistical theory to explain their reported vibrational product distributions and concluded that 20-25% of the energy released goes to translation and rotation and the remainder goes to vibration, which is not especially consistent with a long-range model. However, some reservation should be retained about the role of possible product vibration relaxation in the Thrush and Thomas work, which could result in less than the initial vibrational energy being observed. There is still need for reliable state-to-state data for the E-V energy transfer reactions of $O_2(b)$ and $O_2(a)$ in order to test existing and to develop new models.

II. EXPERIMENTAL TECHNIQUES

a. FLOW REACTORS

The experimental apparatus was a versatile flow reactor pumped with a Roots blower and a mechanical pump. The flow speed could be varied from ∿100 m/s to ∿1 m/s by turning off the Roots blower and throttling the flow to the mechanical pump. Three different flow reactors were used for various experiments (Fig. 1). The initial product distributions measurements for reactions (1) and (2) were done in the flow reactor of 40-mm diameter and 20-cm length. The reactor had two mutually perpendicular windows (quartz) in order to simultaneously measure the emission from $O_2(a)$ and $O_2(b)$; a third window (NaCl) opposite the one for $O_2(b)$ was used for infrared (IR) emission. The reagents were added to the flow reactor close to the IR emission monitoring window via a stainless steel circular ring of 25-mm diameter. The ring was 1.5 cm from the center of the monitoring window, which corresponds to a reaction time of ∿0.2 ms at the best pumping speed (80 m/s^{-1} with blower operating) and 1.5 ms (10 m s with blower not operating). The pressure in the reaction zone was monitored with a MKS Baratron pressure transducer (0-10 torr). For some experiments the flow reactor was connected to a 70-mm inner diameter (i.d.) prereactor 100 cm long, as shown in I of Fig. 1.

The singlet molecular oxygen was produced by a microwave discharge in a 12-mm-i.d. Pyrex tube, which was connected either to the prereactor or directly to the flow reactor itself as in Fig. 1(III). The O_2 flow was passed over Hg heated to ∿50°C Tests showed no appreciable O atom concentration in the discharged O_2 flow in the reaction zone. A chemical generator for singlet oxygen also was available, and some experiments were done in which the chemical generator replaced the microwave discharge source. The design for our chemical generator is the same as that given in Reference 5. Experiments with the chemical generator are not discussed in this report. The prereactor configuration was intended for study

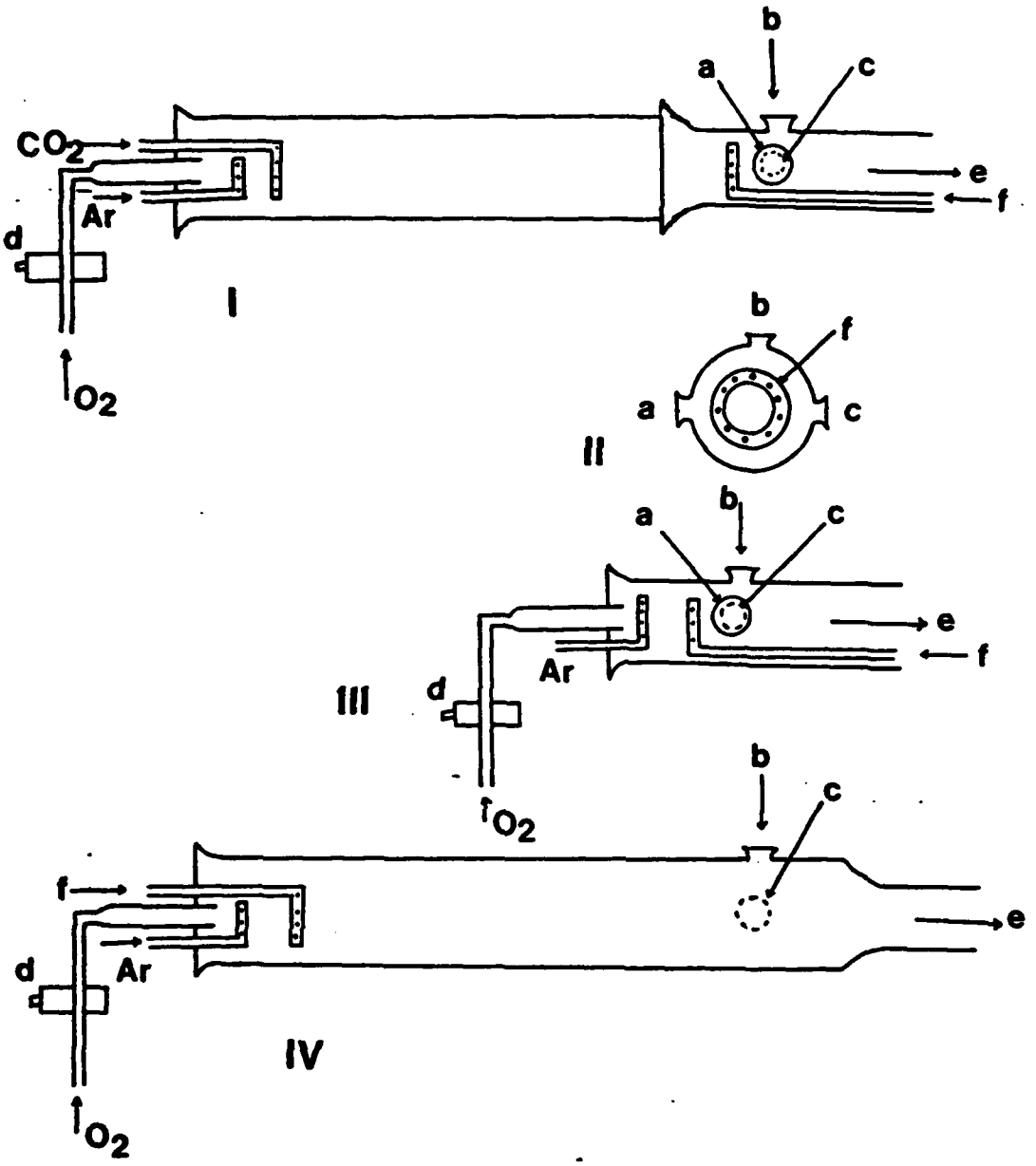

NOTE:
a. FT Spectrometer
b. $O_2(^1\Delta_g)$ detector
c. $O_2(^1\Sigma_g^+)$ detector
d. microwave discharge
e. pumps
f. reagent inlets

Fig. 1. Flow reactor used for study of $O_2(a^1\Delta_g)$ + HF and quenching of $O_2(b^1\Sigma_g^+)$ = (I). (The cross-sectional view of the flow tube, showing the arrangement of the three detectors--(II). Flow reactor used for the E-V measurements with $O_2(b^1\Sigma_g^+)$ - (III). Flow reactor for the quenching rate constant measurement of $O_2(a^1\Delta_g)$ - (IV).)

of the product distributions from $O_2(a)$ reactions; the $[O_2(b)]$ was adjusted by adding CO_2 to the prereactor. This physical arrangement also was used to estimate the quenching rate constants of $O_2(b)$ from perturbation of the steady-state $[O_2(b)]$ concentration by the introduction of reagent to the 40-mm flow reactor (with the inlet tube moved further upstream than for the product studies). For study of the product distribution from the $O_2(b)$ reactions, the prereactor was removed and the singlet O_2 flow was added directly to the 40-mm-diameter flow reactor in order to maximize the $O_2(b)/O_2(a)$ concentration ratio. The arrangement is shown in Figure 1-(III). The quenching rate constants for $O_2(a)$ were measured in a flow tube 140 cm long and 70 mm in diameter, Figure 1-(IV). The typical pumping speed for the $O_2(a)$ quenching measurements was 0.5 m/s; the reagent was added as close to the entrance of the reactor as possible so that a long contact time could be achieved. In order to achieve reliable results with acidic compounds it was necessary to coat the walls of the reactor with a fluorocarbon wax.

b. $O_2(b^1\Sigma_g^+)$ DETECTOR

The fluorescence signal from the $O_2(b^1\Sigma_g^+ - X^3\Sigma_g^-)$ transition at 762.0 nm is proportional to the relative concentration of $O_2(b)$. This emission was collected from the flow tube and focused on the entrance slit of a Jarrell Ash 0.5-m monochromator. A cooled RCA-C31034 photomultiplier tube was attached to the exit slit of the monochromator to measure the fluorescence signal. The signal from the PMT was monitored with a picoammeter.

c. $O_2(a^1\Delta_g)$ DETECTOR

The $O_2(a^1\Delta_g)$ concentration was measured from the $O_2(a^1\Delta_g - X^3\Sigma_g^-)$ emission intensity using an intrinsic germanium detector, Applied Detector Corporation model no. 403. The detector was cooled to liquid nitrogen temperature one hour before operation. A biasing voltage of -250 V was applied from a stabilized D.C. power supply, and the preamplifier was powered by ±12 V from dry cell batteries.

A 8.6-nm band-pass filter peak transmission at 1.27 μm was placed between the detector and flow tube window and the emission was chopped with a Princeton Applied Research (PAR) chopper. The preamplified signal was fed to a PAR HR-8 Lock-in-Amplifier and its output was monitored with a digital voltmeter. The $O_2(a)$ detector and flow reactor were calibrated for absolute $O_2(a)$ concentration by taking the detector and flow reactor to Aerospace Corporation and doing the calibration with known $[O_2a^1\Delta_g]$. The calibration factor was $7.0 \pm 0.4 \times 10^{13}$ molec/cm^3 per mV of signal.

d. FOURIER TRANSFORM INFRARED SPECTROMETER

The infrared chemiluminescence emission intensity from the products of reactions (1) and (2) were monitored with a FT-IR spectrometer (Digilab). The IR emission from the flow reactor was collimated with appropriate optics before it entered the interferometer. The output of the interferometer is focused on an InSb detector cooled to liquid N_2 temperature. The signal from the detector is recorded and processed by a dedicated computer. The operation and calibration of this FT-IR spectrometer has been described elsewhere (Refs. 3,6).

e. REAGENTS, CARRIER GASES AND FLOW CALIBRATIONS

The Ar and O_2 flow rates were monitored with calibrated floating ball-type flow meters and controlled with stainless steel needle valves. The Ar and O_2 were taken from tanks of standard commercial purity and purified by flowing the gases through two molecular sieve-filled traps at 195°C at 1 atm pressure, followed by a molecular sieve trap for Ar at 77 K, and a glass-bead-filled trap at 77 K for O_2. The flowmeters for O_2 and Ar were calibrated for a particular backing pressure, which was subsequently maintained for all experiments. The flow meters were calibrated for a range of gas flows by monitoring the pressure rise in a 12.8-liter vessel for a given time period for a certain flow setting. The increase of pressure with time was linear, and the slope, combined with the gas law, generated

an empirical calibration curve for each flow meter. These original calibration curves were repeatedly verified by simply measuring the increase of pressure in the calibration vessel for a definite time for a given flow setting.

Most reagent flow rates were measured for each experiment by monitoring the increase of pressure in a 5-liter calibrated volume for a given needle valve setting. Two exceptions to this were HF and CO_2. Since large quantities of these reagents were required, these gases were taken directly from Matheson tanks and each line had its own flow monitor system. The CO_2 flow line had a floating ball-type flow meter, which was calibrated in the same way as described for the O_2 and Ar flow meters. The HF cylinder was cooled to 0° to reduce the vapor pressure to 320 torr, so that the flow rate was in the desired range for the needle valve that was placed in the line. The HF flow rates were measured by observing the pressure rise in a 10.8-liter stainless steel reservoir using a MKS Baratron pressure transducer (0-10 torr). The HF was transferred to the flow reactor using entirely stainless steel lines and valves.

Most of the other reagents were taken from Matheson lecture bottles. Since either high concentrations or long signal averaging periods were required, large quantities of reagent gases were needed. Therefore, extensive purification procedures were not practical, except for freeze/thaw-pump cycles to remove volatile impurities. Care was taken to remove Br_2 and I_2 impurity from HBr and HI. The reagents were stored as gases in 10-liter Pyrex reservoirs prior to experiments. Since rate constants generally are small for all small stable molecules, minor impurities should be of no consequence.

III. RESULTS

a. QUENCHING RATE CONSTANTS FOR $O_2(b)$

We used the flow reactor with the prereactor geometry of Figure 1-(I) to measure the quenching of $O_2(b)$. The roots blower was not used for these experiments and the $[O_2(a)]$ was 3.0×10^{15} molec cm^{-3} s^{-1}. Upon reaching the reagent inlet of Figure 1-(I), the $[O_2(b)]$ was in steady-state with $[O_2(a)]$ because of the quenching by the wall and by H_2O impurity. The reagents were added 5-10 cm in front of the observation window and the decline in $[O_2(b)]$ emission intensity was monitored. The distance was varied and the longer distance was used for reagents with the smaller rate constants. The decay of $[O_2(b)]$ followed first-order kinetics for ~60% decrease in $[O_2(b)]$ for most reagents. The extent of first-order decay is governed by the tendency to establish a new steady-state $[O_2(b)]$. First, the rate constants were measured for several reagents previously studied and the results were in moderately good agreement with the published rate constants. Therefore, the measurements were extended to reagents of interest to the KSU work. The results of this report are considered as preliminary and reliable to within a factor of ~2. Soon these reactions will be reinvestigated using a movable detector technique to identify any concentration dependent wall deactivation rate processes and to better characterize the decay before the development of the new steady-state.

The rate constants measured in the present work, and other reported values are given in Table 1. One objective, which was not realized, was to find a reagent that had a large rate constant for quenching $O_2(b)$ but not for $O_2(a)$. Such a reagent would permit the $O_2(b)/O_2(a)$ ratio to be reduced using a prereactor so that reaction (2) could be isolated. The current best choice for such a reagent seems to be CO_2; but the $O_2(b)$ quenching is still slow enough so that rather large quantities of CO_2 are required and significant vibrational relaxation of product molecules from reaction (2) may occur for some reagents.

TABLE 1. RATE CONSTANTS FOR QUENCHING OF $O_2(b^1\Sigma_g^+)$ AT 300 K

Reagent	k_Q^b 10^{-14} cm^3 MOL^{-1} s^{-1}	Reference
HF	110 ± 20	This work
HCl	4.0 ± 2.0	This work
	7.2 ± 0.17	10a
	2.66 ± 0.38	12d
	6.7 ± 3.5	28
	13.0 ± 4.0	16
HBr	20 ± 4	This work
	38	19b
HCN	8.0 ± 2.0	This work
COS	2.3 ± 1.0	This work
	5.5 ± 3.5	28
CH_3Cl	80 ± 40	This work
H_2S	20 ± 10	This work
	33	27
CO_2	30 ± 10	This work
	34.7 ± 4.7	12d
	30	9b
	50 ± 3	17
	36	25
NH_3	130 ± 20	This work
	117 ± 17	12d
	180	9b
	199 ± 50	10a
	166 ± 20	16
	220	27
H_2	45 ± 20	This work
	92 ± 43	28
	40	9b
	82.4 ± 10.3	16
H_2O	500 ± 100	9a
	670 ± 50	15

b. STATE-TO-STATE STUDIES FOR $O_2(b^1\Sigma_g^+)$ REACTIONS

These studies were done without the prereactor, and the singlet oxygen was added directly to the 4.0-cm-diameter flow reactor, Figure 1-(III). This geometry maximized the $O_2(b)/O_2(a)$ concentration ratio and ensured that the contribution from $O_2(a)$ quenching to the observed IR emission was negligible. The pumping speed was adjusted from nearly the highest possible speed (for HF) to highly throttled conditions of the blower plus mechanical pump. Relative to the configuration with the prereactor, the $O_2(b)/O_2(a)$ ratio was increased by a factor of $\sim$10 with the absolute $[O_2(a)]$ being $\sim 2 \times 10^{15}$ molec cm^{-3}. In the KSU apparatus $[O_2(b)]$ was generated by the microwave discharge, as well as by energy pooling, and the highest $[O_2(b)]$ was for the shortest flow time from the discharge to the observation point. For these operating conditions, the $[O_2(b)]$ was directly proportional to the O_2 flow rate and to the discharge power. In order to minimize vibrational relaxation, the O_2 (and reagent) flows were reduced as much as possible. Experiments were done at constant pressure, 0.8 torr, with replacement of as much O_2 with Ar as was possible and still observe IR emission.

For the hydrogen halide series, the IR emission intensity was always first-order in $[O_2(b)]$ and [HX]; see Figure 2. Furthermore, the relative product concentrations (relative intensities divided by Einstein coefficients) were in close agreement with relative quenching rate constants measured in the preceding section. This suggests that formation of HX(v=0) probably is not an important product channel for reaction (1).

1. Reaction with HF

Since HF has the largest Einstein coefficient and the largest quenching rate constant, the HF reaction could be studied at the lowest concentration and shortest contact time of any reagent. For a contact time of 0.25 ms and for $[HF] = 10^{12} - 10^{13}$ molec cm^{-3} and $[O_2] = 5 \times 10^{15}$ molec cm^{-3}, emission from only HF(v=1) could

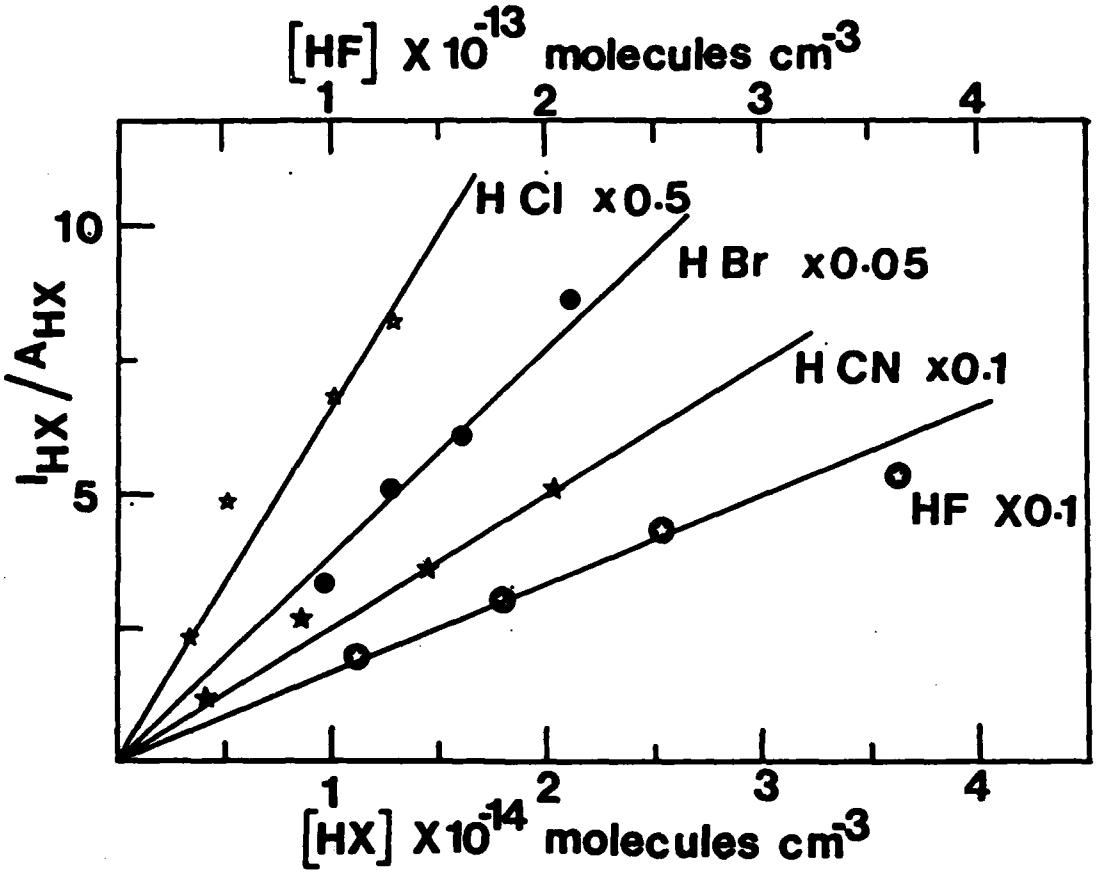

Fig. 2. Relative HX(v) concentration from $O_2(b)$ reactions vs. reagent concentration: $[O_2] = 1.1 \times 10^{16}$, $[O_2(a^1\Delta_g)] = 1.4 \times 10^{15}$, $[Ar] = 1.3 \times 10^{16}$ molec cm^{-3} and $\Delta t = 0.67$ ms. (The factors denote the reduction in the I_{HX} values prior to making the plot.)

be observed. Not even trace amounts of HF(v=2) emission were present. Modeling studies for these flow conditions (including vibrational relaxation by both HF and O_2) suggest that vibrational relaxation should be modest. The degree of relaxation was checked by adding I_2 to the system to generate $I(^2P_{\frac{1}{2}})$ atoms. The $I(^2P_{\frac{1}{2}})$ reaction with HF generated an observable HF(2) concentration. Changing the HF and O_2 concentrations in the I_2 system over the same range as used to study $O_2(b)$ and HF did affect the HF(2)/HF(1) ratio; thus, if HF(2) was formed from reaction (3), it should have been observed. We conclude that quenching of $O_2(b)$ by HF generates mainly HF(1), with perhaps lesser amounts of HF(0), and that the reaction proceeds as follows.

$$\begin{aligned} O_2(b^1\Sigma_g^+) + HF &\rightarrow O_2(a^1\Delta_g) + HF(1) \quad \Delta H_o^\circ = -1280 \text{ cm}^{-1} \\ &\rightarrow O_2(a^1\Delta_g) + HF(0) \quad \Delta H_o^\circ = -5239 \text{ cm}^{-1} \end{aligned} \tag{3}$$

2. Reaction with HCl

The smaller rate constant and Einstein coefficient for HCl relative to HF required both slower pumping speed and higher HCl concentrations than for $O_2(b)$ + HF. The HCl emission could be studied for $[O_2] = 1.1 \times 10^{16}$ and $[HCl] = 10^{13} - 10^{14}$ molec cm^{-1} for a contact time of 0.67 ms (Fig. 3). The emission was mainly from HCl(1), although some HCl(2) could be observed; the HCl(1)/HCl(2) ratio was 9 and appeared to be independent of [HCl] over the 10^{13} to 10^{14} molec cm^{-3} range. Although the model calculations, which included relaxation by HCl and O_2, suggest that some HCl(2) relaxation may have occurred under these conditions, the evidence strongly favors the following reactions for quenching of $O_2(b)$, with reaction 4b being dominant at 300 K.

$$\begin{aligned} O_2(b^1\Sigma_g^+) + HCl &\rightarrow HCl(2) + O_2(a^1\Delta_g) \quad \Delta H_o^\circ = 429 \text{ cm}^{-1} \quad \text{(a)} \\ &\rightarrow HCl(1) + O_2(a^1\Delta_g) \quad \Delta H_o^\circ = -2353 \text{ cm}^{-1} \quad \text{(b)} \end{aligned} \tag{4}$$

The results in the next section for HBr also support the claim that if relaxation had been extensive, it would have been detected as a variable HCl(2)/HCl(1) ratio

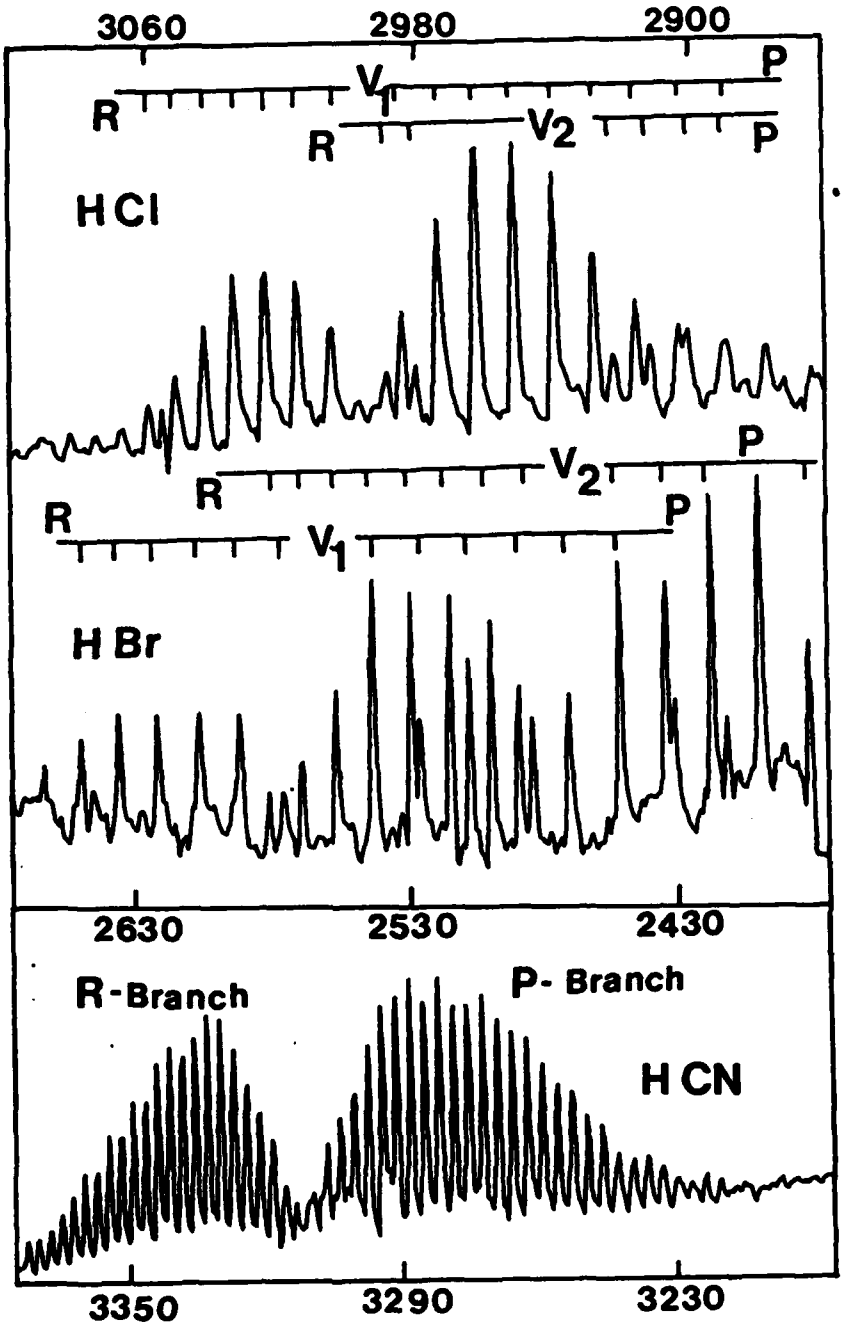

Fig. 3. Emission spectra from the reactions of $O_2(b^1\Sigma_g^+)$ for $[O_2] = 1.1 \times 10^{16}$, $[O_2(^1\Delta_g)] = 1.4 \times 10^{15}$, $[Ar] = 1.3 \times 10^{16}$ molec cm^{-3} and $\Delta t = 0.67$ ms ([HCl], [HBr] and [HCN] = 2.0, 2.5 and 2.0×10^{14} molec cm^{-3}, respectively.)

when the HCl concentration was changed.

3. Reaction with HBr

The $O_2(b)$ quenching rate constant by HBr is $\sim 1 \times 10^{-13}$ cm^3 $molec^{-1}$ sec^{-1}, which is about 3 times higher than for HCl. Since the Einstein coefficient for HBr is about 5 times smaller than that of HCl, the HBr spectra from the HBr reaction had about the same intensity as that from HCl (Fig. 3). We used a pumping speed of 30 m/s i.e., the contact time was 0.67 ms, the [HBr] was 0.4-2 $\times 10^{14}$ molec cm^{-3} for $[O_2] = 1.2 \times 10^{16}$ molec cm^{-3}. As the [HBr] was decreased from 2.0-1.0 $\times 10^{14}$ molec cm^{-3}, there was a small change in the HBr(2)/HBr(1) ratio; however, further reduction of [HBr] gave a distinct increase in HBr(2)/HBr(1) and at 0.4×10^{14} molec cm^{-3} the ratio was ~ 2.5. Extrapolation of the curve in Fig. 4 to zero [HBr] suggests an initial HBr(2)/HBr(1) ratio of ~ 3.5.

Since some relaxation of HBr(v=2) may still exist in the extrapolated ratio of Fig. 4 because of collisions with O_2, the HBr(2)/HBr(1) ratio versus [HBr] was studied at different $[O_2]$. For the higher $[O_2]$, 1.9×10^{16} molec cm^{-3}, and a contact time of 0.67 ms, the extrapolated ratio was ~ 2. The product distribution at a pumping speed of 50 m/s, which gives a reaction time of 0.4 ms with $[O_2] = 8 \times 10^{15}$ molec cm^{-3} also was studied. The spectra were somewhat noisy, but the data could be analyzed. Extrapolation to zero [HBr], Fig. 4, gave a ratio of ~ 4. We conclude that the initial HBr(2)/HBr(1) ratio should be close to 4 and that $O_2(a^1\Delta_g)$ must be the final O_2 state from reaction of $O_2(b)$ with HBr.

$$\begin{aligned} O_2(b^1\Sigma_g^+) + HBr &\rightarrow HBr(2) + O_2(a^1\Delta_g) \quad \Delta H_\circ^\circ = -210 \text{ cm}^{-1} \\ &\rightarrow HBr(1) + O_2(a^1\Delta_g) \quad \Delta H_\circ^\circ = -2679 \text{ cm}^{-1} \end{aligned} \tag{5}$$

4. Reaction with HCN

The emission spectrum from the reaction of $O_2(b)$ with HCN is shown in Fig. 3. The reaction has a quenching rate constant of $\sim 0.8 \times 10^{-13}$ cm^3 $molec^{-1}$ sec^{-1}. The [HCN] was changed from 2.3 to 14 $\times 10^{13}$ molec cm^{-3} for a contact time of

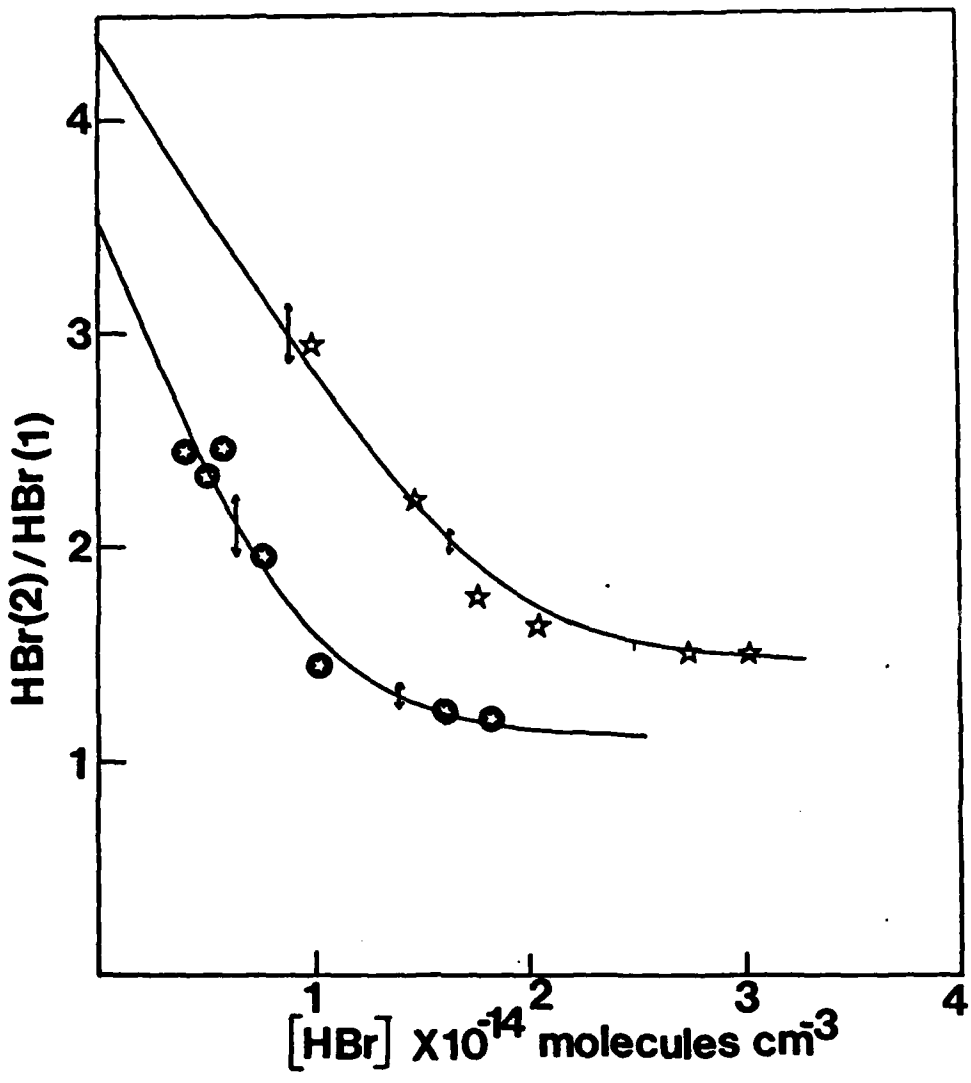

NOTE: ☆-$[O_2]$, [Ar] and $[O_2(a)]$ = 8.0 x 10^{15}, 1.6 x 10^{16} and 1.3 x 10^{15} molec cm^{-3} for Δt = 0.4 ms ✪ $[O_2]$, [Ar] and $[O_2(a)]$ = 1.2 x 10^{16}, 1.3 x 10^{16} and 2.4 x 10^{15} for Δt = 0.67 ms. The vertical arrows indicate the experimental uncertainty from the spectral analysis.

Fig. 4. The variation of the HBr(2)/HBr(1) ratio vs. [HBr) from the $O_2(b)$ reaction.

0.67 ms and $[O_2]$ = 1.1 x 10^{16} molec cm^{-3}. For all conditions, only the HCN(001-000) transition was observed. There is sufficient energy to excite the $\nu_3 + \nu_2$ levels; however, careful searches failed to identify HCN(021-020) or HCN(011-010) emissions. Since the energy match between $2\nu_2$ and ν_3 (or ν_1) is not close for HCN, it is unlikely that relaxation of HCN(021) or HCN(011) by collisions with either HCN or O_2 would have been complete for our experimental conditions. The bending mode apparently is not extensively excited in quenching of $O_2(b)$ by HCN. Thus, the main reaction should be

$$O_2(b^1\Sigma_g^+) + HCN \rightarrow O_2(a^1\Delta_g) + HCN(001) \qquad \Delta H_\circ^\circ = -1927\ cm^{-1} \qquad (6)$$

5. Reaction with NO

The NO emission could be observed only with slow pumping speeds and high [NO]. For a pumping speed of 10 m/s, which corresponds to a reaction time of 2.0 ms and [NO] = 1 10^{15} molec cm^{-3}, we observed mainly NO(v=1) with a trace of NO(v=2). For these experimental conditions, the initial NO(v) distribution almost certainly was relaxed and no conclusion can be made about the initial NO(v) product states. The final O_2 product state was probably $O_2(a^1\Delta_g)$.

6. Reaction with CO_2

Since the CO_2 rate constant is large, 3 x 10^{-13} cm^3 $molec^{-1}$ sec^{-1}, and the Einstein coefficient is favorable, the interferometer was purged with N_2 in order to reduce the absorption by atmospheric CO_2, and an attempt was made to record the CO_2 IR emission. Emission from CO_2(001-000) could be observed easily, but, the atmospheric absorption of the CO_2(001-000) band could not be totally removed. Thus, the spectrum was very distorted with the emission from the CO_2 levels with high Boltzmann populations being absorbed. The observed CO_2(001-000) spectra showed isotopic lines from $C^{13}O_2$ and $CO^{16}O^{18}$ emission, and strong emission from high J lines of $C^{12}O_2{}^{16}$. The lowest pressure, and smallest contact time corresponded to a reaction time of 0.67 ms with $[CO_2]$ = 3.6 x 10^{13} molec cm^{-3} and

$[O_2] = 1.2 \times 10^{16}$ molec cm^{-3} s^{-1}. For this condition, emission from $CO_2(001)$, only, was observed.

As for HCN, enough energy exists to produce simultaneous excitation of several other levels and CO_2(041; 121; 201 and 002) are all close to resonance. However, no emission from these levels could be observed. Inspection of vibrational relaxation data for $CO_2(021)$ and $CO_2(101)$ by CO_2 and O_2 suggests that the relaxation times would be < 1 ms. Thus, relaxation probably is serious, and $CO_2(021)$ and $CO_2(101)$ or the energy resonant levels cannot be excluded as initial product states. The $CO_2(002)$ state may relax very rapidly. Nevertheless, if only the energy resonent levels were initial products, it seems that some emission should have been observed from those levels. Since this was not the case, the energy may be distributed among several levels which relax to $CO_2(001)$.

c. RATE CONSTANT MEASUREMENTS FOR $O_2(a^1\Delta_g)$

The quenching rate constants of $O_2(a)$ are very small. Therefore, slow flow rates (long contact times) and high reagent concentrations are required to obtain appreciable quenching of $[O_2(a)]$. A 7-cm-diameter Pyrex tube was used with Ar and O_2 concentrations of 5 and 0.5 torr, respectively, with typical contact times of 3.0 sec; see Figure 1-(IV). Even for these slow flow conditions, $[O_2(a)]$ was $\sim 3 \times 10^{15}$ molec cm^3, because the quenching at the wall for $O_2(a)$ is minimal. The rate constants were measured for pseudo first-order conditions with the fixed observations point method. Assuming that quenching is fast enough to be observed for reasonable reagent concentrations, the largest source of error in this method is the possible development of a wall deactivation rate constant that depends on the reagent concentration, i.e., the surface may be activated by absorption of reagent molecules. The literature mentions such problems for $O_2(a)$ quenching by acidic or basic reagent molecules. Several sample quenching plots are shown in Figure 5. No difficulties were encountered for such cases as NO, C_4H_6, CH_3I

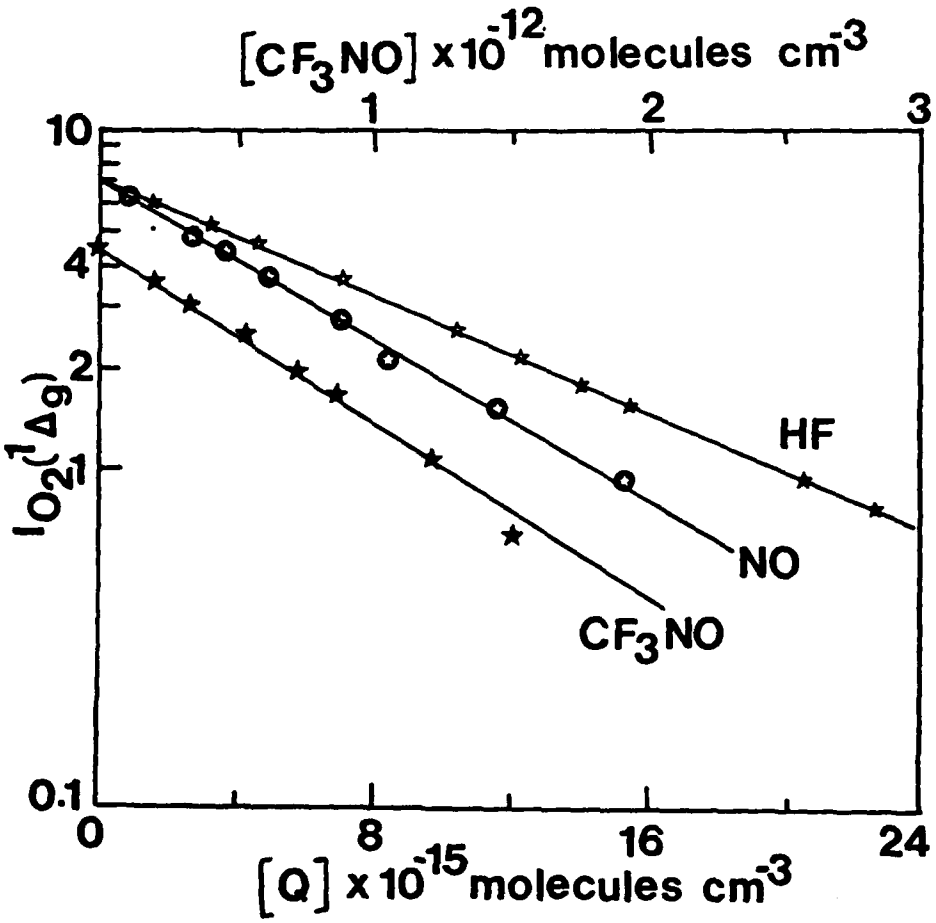

NOTE: (a) HF(★) with $[O_2]$ and [Ar] = 2.9 x 10^{16} and 15.7 x 10^{16} molec cm^{-3} with Δt = 1.1 sec; (b) NO(✪) with $[O_2]$ and [Ar] = 2.9 x 10^{16} and 13.0 x 10^{16} molec cm^{-3} for Δt = 5.2 sec; and (c) CF_3NO(★) with $[O_2]$ and [Ar] = 0.7 x 10^{16} and 2.8 x 10^{16} molec cm^{-3} for Δt = 0.5 sec.

Fig. 5. Quenching plots for $O_2(a^1\Delta_g)$.

TABLE 2: QUENCHING RATE CONSTANTS[a] FOR $O_2(a^1\Delta_g)$ at 300 K

Reagent	k_Q 10^{-18} cm^3 molec^{-1}s^{-1}	Reference
HF	150 ± 75	This work
HCl	4 ± 4	This work
	130	12d
HBr	8 ± 4	This work
HCN	5 ± 2	This work
Cl_2	6 ± 3	This work
NO	50 ± 10	This work
	35	12d
	45	9a
NH_3	10 ± 2	This work
	8.9	
	4.4	9b
COS	2.0 ± 1.0	This work
CO	9 ± 4	This work
	8.6	10a
CO_2	<0.5	This work
	<0.01	9a
	<0.36	13
H_2S	2 ± 2	This work
CH_3Cl	5 ± 5	This work
CH_3I	40 ± 20	This work
CH_3Br	30 ± 15	This work
CF_3Br	<0.5	This work
CF_3I	<0.5	This work
CF_3NO	$3.0 \pm 1 \times 10^6$	This work
C_2N_2	~0.5	This work
C_4H_6	10 ± 10	This work
Cis-C_4H_8	20 ± 10	This work
$(CH_3)_3N$	3000 ± 1000	This work

or CF_3NO. However, nonlinear plots were found for HCl, HBr, and H_2S, which suggest the development of fast rates for wall quenching. No difficulties were encountered for HF, which is the most interesting molecule for E-V transfer studies with $O_2(a)$. In order to study the acidic molecules, it was necessary to coat the walls of the flow reactor with fluorocarbon wax. After this treatment good first order plots were obtained for the acidic molecules and there were no changes for the other reagents. A summary of rate constants is given in Table 2. The quoted error limits include estimates of systematic error, as well as statistical uncertainty.

The most unusual aspect of Table 2 is the very large quenching rate constant for CF_3NO. This was checked repeatedly and verified. Since CF_3I and other similar molecules have small rate constants, the quenching mechanism must be specific for CF_3NO. One possibility is E-E transfer rather than E-V transfer. This possibility was confirmed by observing an <u>increase</u> in emission intensity with the intrinsic germanium detector (without the filter) when CF_3NO was added to the flow. Based upon the relative HF and HCl emission intensities, the smaller HCl quenching rate constant found in this work is preferred over that of Reference 12d. Nevertheless, surface interactions may render both measurements somewhat unreliable. In general the small quenching rate constants for HCl, HBr and HCN are consistent with the absence of any emission from quenching of $O_2(a)$.

D. E-V TRANSFER FROM $O_2(a^1\Delta_g)$ TO HF

In a previous section, the E-V transfer from $O_2(b)$ to HF was characterized by using an experimental arrangement that maximized the $O_2(b)/O_2(a)$ ratio. Now we wish to reverse this situation and minimize $O_2(b)/O_2(a)$ but still have a high $[O_2(a)]$. This was done by placing the prereactor in front of the IR emission reactor and adding variable quantities of CO_2 to reduce the steady-state $O_2(b)$ concentration. The objective is to isolate reaction (7) in the presence of reaction (3).

$$O_2(a^1\Delta_g) + HF \rightarrow HF(2) + O_2(X^3\Sigma_g^-) \quad \Delta H^\circ = -146\ cm^{-1} \quad a.$$
$$\rightarrow HF(1) + O_2(X^3\Sigma_g^-) \quad \Delta H^\circ = -3924\ cm^{-1} \quad b. \qquad (7)$$
$$\rightarrow HF(0) + O_2(X^3\Sigma_g^-) \quad \Delta H^\circ = -7882\ cm^{-1} \quad c.$$

The HF quenching rate constants are 1.1×10^{-12} and 1.5×10^{-16} cm^3 $molec^{-1}$ s^{-1} for $O_2(b)$ and $O_2(a)$, respectively. Thus, the $O_2(a)/O_2(b)$ ratio must be $\sim 10^4$ to observe reaction (8). Adding CO_2 does remove $O_2(b)$, $k^b_{CO_2} = 5 \times 10^{-13}$ cm^3 $molec^{-1}$ sec^{-1}, without removing $O_2(a)$, $k^a_{CO_2} \leq 5 \times 10^{-19}$ cm^3 $molec^{-1}$ s^{-1}. Although one must consider the deactivation of HF(2) and HF(1) by the CO_2, the major problem in studying reaction (7) is the self-relaxation by the [HF] required to generate observable HF(v) product.

We first demonstrated the first-order dependence of the HF(1-0) emission intensity upon [HF] for the prereactor geometry. The HF(2-1) emission intensity, although observable, was too weak to be important for these kinetic studies. Some typical results are shown in Figure 6 for both high (80 ms^{-1}) and low (10 ms^{-1}) flow velocities. The high flow velocity is required to reduce HF(v) relaxation, and all further work was for this condition which has a 0.2 ms HF contact time; the concentrations were $O_2(a)$, $O_2(X)$ and Ar = 3.5×10^{14}, 4.2×10^{15} and 3.1×10^{16} molec cm^{-3}, respectively. In the next experiments, [HF], $[O_2(X)]$ and [Ar] were fixed at 3×10^{14}, 8.2×10^{15} and 7.4×10^{16} molec cm^{-3}, and $[O_2(b)]$ was changed by adding CO_2. Data were collected for $[O_2(a)]$ = 4.5, 5.6, 6.7 and 7.4×10^{14} molec cm^{-3}. The somewhat lower $[O_2(a)]$ in this work, relative to values quoted in other parts of this report, are a consequence of the use of the maximum flow velocities. The linear I_{HF} versus relative $[O_2(b)]$ plots of Figure 7a were extrapolated to $[O_2(b)] = 0$ to obtain the I_{HF} from only reaction (7). These intercepts are plotted in Figure 7b versus $[O_2(a)]$, and a linear relationship is obtained. These experiments seem to demonstrate that both $O_2(b)$ and $O_2(a)$ reac-

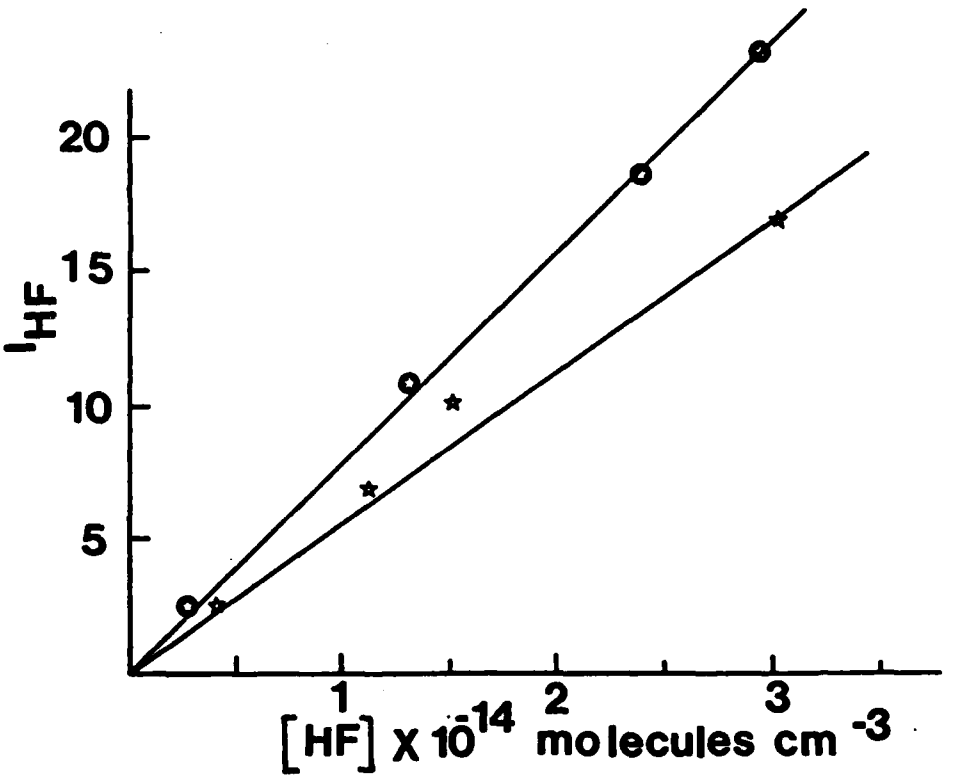

NOTE: (●) Slow pumping speed (Δt = 1.2 msec) for $[O_2] = 2.0 \times 10^{16}$, $[O_2(a)] = 2.8 \times 10^{15}$ and $[Ar] = 1.0 \times 10^{16}$ molec cm^{-3} (★) High pumping speed (Δt = 0.2 msec) for $[O_2] = 4.7 \times 10^{15}$ $[O_2(a)] = 3.5 \times 10^{14}$, $[Ar] = 2.1 \times 10^{16}$ molec cm^{-3}.

Fig. 6. HF emission intensity in arbitrary units vs. [HF].

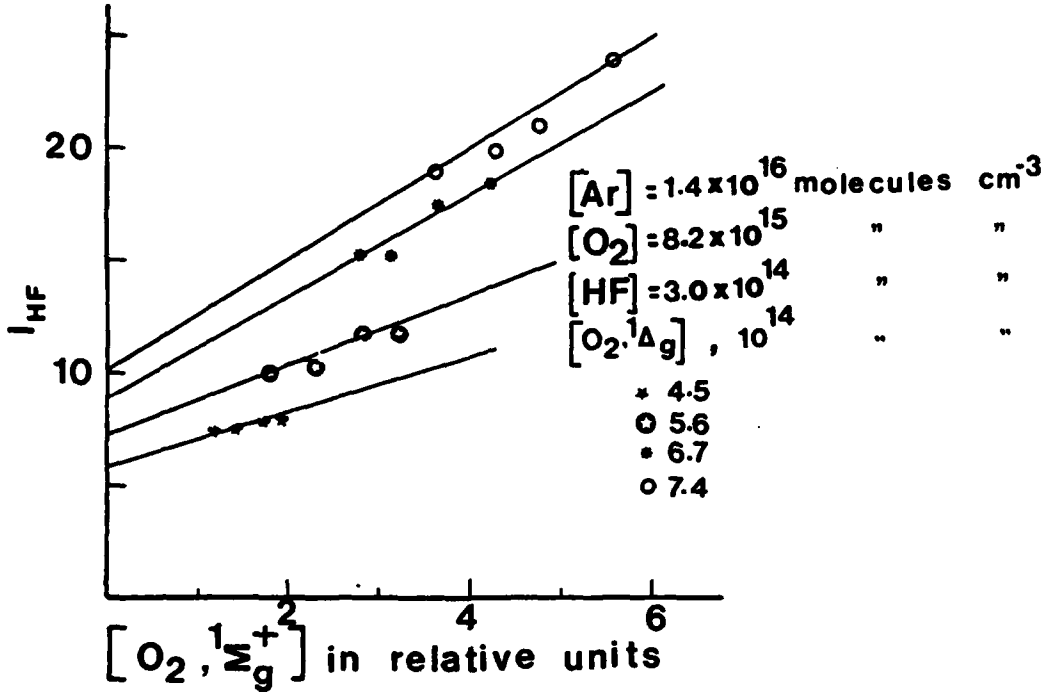

NOTE: All data are for an HF contact time of 0.2 msec. The O_2(b) was reduced by addition of CO_2 to the prereactor. The CO_2 reaction time was sufficiently long to set up the steady-state between O_2(a) and O_2(b) and the CO_2 concentration range extended to 7.0×10^{13} molec cm^{-3}.

Figure 7a. The dependence of I_{HF} on $[O_2(b)]$ for various $[O_2(a)]$.

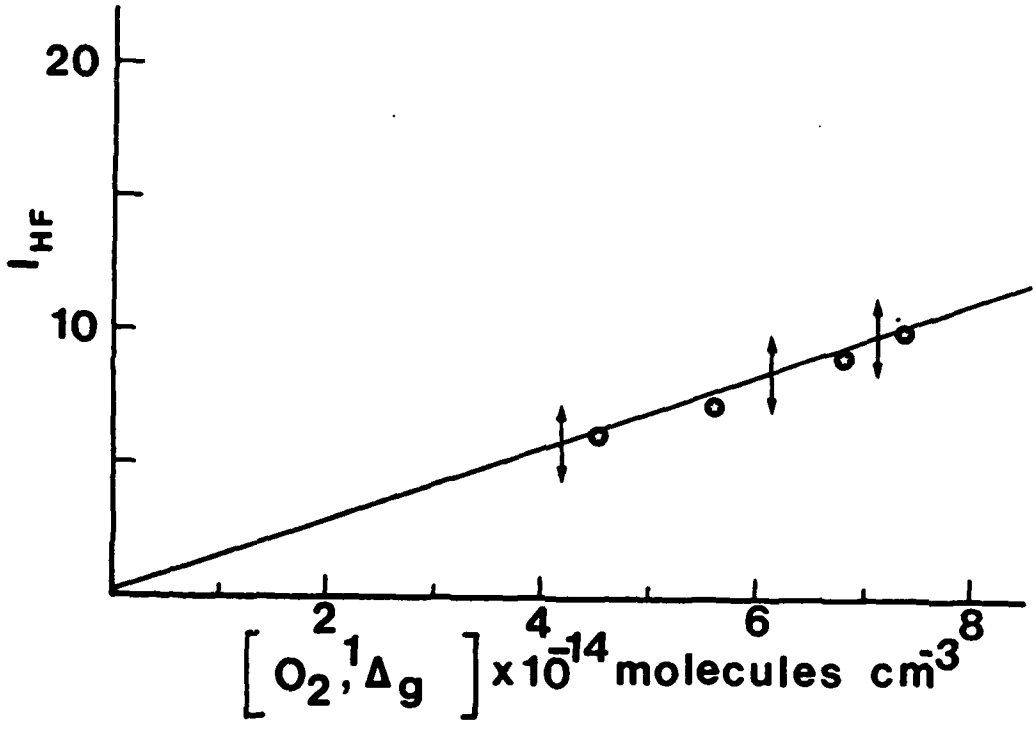

Fig. 7b. The intercepts in Fig. 7a vs. the corresponding $[O_2(a^1\Delta_g)]$.

tions are contributing to the HF(1-0) emission intensity for these particular experimental conditions. The approximate $O_2(a)$ and $O_2(b)$ concentrations are evaluated next to see whether or not the conclusions based on Figure 7 are consistent with the HF quenching rate constants.

If the total quenching rate constants are assigned as E-V transfer, then the data of Figure 7 can be used to get $[O_2(b)]$.

$$\frac{I^a_{HF}}{I^b_{HF}} = \frac{k^a_{HF}[O_2(a)]\Delta t}{k^b_{HF}[O_2(b)]\Delta t} \tag{8}$$

The intercepts from Figure 7a correspond to I^a_{HF}, and the total intensity (with no added CO_2) less the intercept values gives I^b_{HF}. This ratio is approximately unity for $[O_2(a)] = 6.7 \times 10^{14}$ molec cm^{-3}. Combining these results and the rate constants of Tables 1 and 2 give $[O_2(b)] \approx 1.0 \times 10^{11}$ molec cm^{-3}. This may be compared with the steady-state prediction, Equation 9.

$$[O_2(b)] = \frac{k_{EP}[O_2(a)]^2}{k_{H_2O}[H_2O] + k_{wall}} \tag{9}$$

The $O_2(b)$ formation rate is given by the slow energy pooling reaction and the removal rate by the reaction with the wall and with the water (and other) impurity. Our flow tube design is similar to that of Borrell, et al (Ref. 12d), and their formulation suggests $k_w \approx 30$ sec^{-1}. The estimated H_2O concentration in our tank O_2 is 300 p/m. Since these HF experiments were done without purification, the $[H_2O]$ will correspond to $\sim 2 \times 10^{12}$ molec cm^{-3}, which gives $[O_2(b)] \approx 2.3 \times 10^{11}$ molec cm^{-3} according to Equation 9. Considering the large uncertainties in the analysis, the agreement between the two estimates of $[O_2(b)]$ is acceptable. Further confirmation of this range for $[O_2(b)]$ was obtained from the effect of

purifying the O_2 flow. The addition of two dry-ice-cooled molecular sieve traps (at high pressure) and one liquid N_2 cooled glass-bead-filled to the low pressure side of the O_2 line increased $[O_2(b)]$ by ∿3, but $[O_2(a)]$ increased by only ∿30%. This confirms that for the HF emission experiments k_{wall} and $k_{H_2O}[H_2O]$ were comparable. Similar estimates for $k_{H_2O}[H_2O] + k_{wall}$ were obtained by noting the $[CO_2]$ required in the prereactor to reduce $[O_2(b)]$ by a factor of 2.

As a final point, one needs to know the HF(v) distribution from reaction (7). The deactivation rate constants for HF(2) by HF, CO_2, H_2O and O_2 are reasonably well known (Ref. 29) (and the values are 1.9×10^{-11}, 5.2×10^{-12}, 4.0×10^{-10} and 2.4×10^{-14} cm^3 $molec^{-1}$ sec^{-1}, respectively). The critical problem is the quenching by HF which mainly proceeds to give HF(1): $HF(2) + HF(0) \rightarrow 2HF(1)$. An attempt was made to estimate the degree of HF relaxation by doing a series of experiments with variable [HF] and monitoring HF(2)/HF(1). The $[O_2(a)]$, $[O_2(X)]$ and [Ar] were 5×10^{14}, 4.7×10^{15} and 2.1×10^{16} molec cm^{-3} and the contract time was 0.2 msec. An HF spectrum for [HF] = 2×10^{14} molec cm^{-3} is shown in Figure 8. This spectrum corresponds to 512 scans at 4 cm^{-1} resolution; the signal/noise ratio is not high but analysis can be done to give HF(2)/HF(1) = 0.10 ± 0.02. This ratio was constant down to [HF] ≳ 0.6×10^{14} molec cm^{-3}. Experiments for [HF] from $0.6 - 0.3 \times 10^{14}$ molec cm^{-3} suggest that the HF(2)/HF(1) ratio increases to ∿0.2 at the lowest concentration for which reliable spectra could be obtained. For [HF] = 0.3×10^{14} molec cm^{-3}, the relaxation time for HF(2) would be ∿2 msec and most of the relaxation should have been arrested since our observation time was ∿0.2 msec. Since the total HF emission arises from roughly equal contributions of $O_2(a)$ and $O_2(b)$, and since $O_2(b)$ gives exclusively HF(1), these data with HF(2)/HF(1) = 0.2 suggest that reaction (7) may give approximately equal amounts of HF(2) and HF(1).

This tentative conclusion can be checked by examining the HF emission spectra

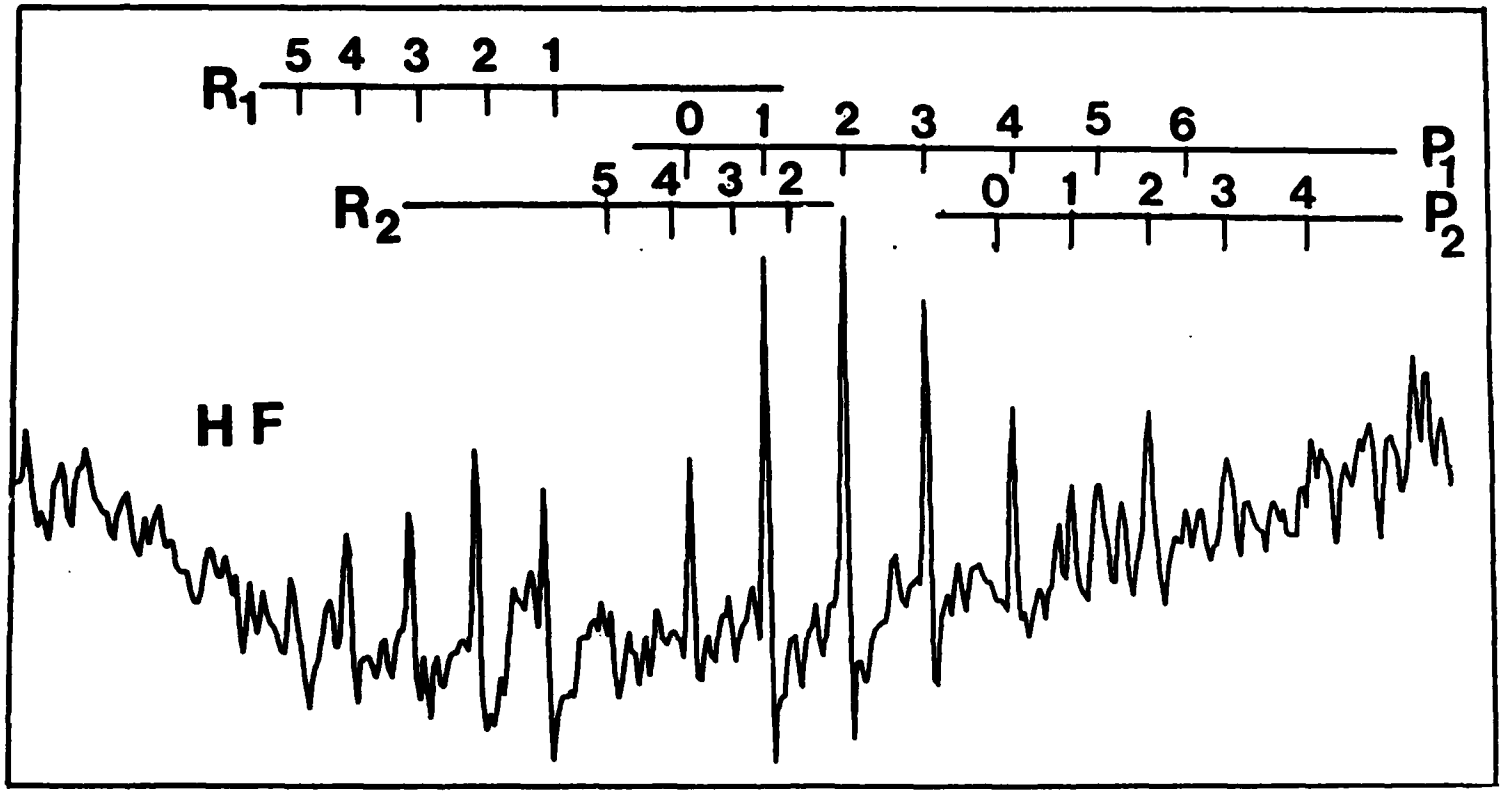

Fig. 8. Emission spectrum from reaction of a mixture of $O_2(a)$ and $O_2(b)$ showing the HF(1-0) and the HF(2-1) Bands for $[O_2] = 4.7 \times 10^{15}$, $[O_2(a)] = 4.5 \times 10^{15}$, $[Ar] = 1.8 \times 10^{16}$ and $[HF] = 2.9 \times 10^{14}$ molec cm^{-3} and $\Delta t = 0.2$ msec.

as CO_2 is added to reduce $[O_2(b)]$. These experiments were done for $[O_2(a)]$ and $[HF] = 5.6 \times 10^{14}$ and 1.5×10^{14} molec cm^{-3} and a contact time of 0.2 msec. Experiments were done with $[CO_2] = 1.7, 5.6, 14$ and 25×10^{13} molec cm^{-3}, which reduced $[O_2(b)]$ by factors of 1.4, 1.8, 3.0 and 6.0. The reduction in the HF(1-0) emission intensity was similar to that for Figure 7a; but, the HF(2)/HF(1) ratio increased only slightly. Although this [HF] probably did cause some HF(2) relaxation, these results still suggest that reactions (7a) and (7b) are of comparable importance. Full-scale computer model calculations support this general conclusion, assuming equal HF(v) contributions from $O_2(a)$ and $O_2(b)$ reactions and including relaxation by H_2O, CO_2, HF and O_2.

V. CONCLUSIONS

Total $O_2(a)$ and $O_2(b)$ quenching rate constants have been measured for the hydrogen halides and HCN using a flowing afterglow technique. The rate constant ratio is $\sim 10^4$ in favor of $O_2(b)$. Since the $O_2(b)/O_2(a)$ concentration ratio for most experimental conditions is $\geq 10^{-4}$, the majority of the IR emission observed from hydrogen halides following E-V transfer reactions from "singlet oxygen" comes from the reactions of $O_2(b)$. One potential problem of a general nature in E-V transfer studies with $O_2(a)$ and $O_2(b)$ can be kinetic complication because of reversibility and presence of a large excess of $O_2(X)$. This was not a problem, however, for $O_2(b)$ because the product state is $O_2(a)$ rather than $O_2(X)$, or for $O_2(a)$ because the relaxation of the vibrationally excited molecules by the parent reagent is generally faster than the reverse of the E-V transfer step with $O_2(X)$.

In the present work, we isolated and observed the E-V transfer reactions of $O_2(b)$ with HF, HCl, HBr and HCN at the state-to-state level. Based upon the observed product states, we conclude that the quenching of $O_2(b)$ gives $O_2(a)$ and not $O_2(X)$ in each case. As inferred by other workers (Ref. 19), this difference in final product state is probably the main reason that the quenching of $O_2(b)$ is faster than $O_2(a)$ for simple E-V physical quenching. These state-to-state data do not necessarily support an energy resonance mechanism for E-V quenching of $O_2(b)$. In fact, the reagent (HF) with the largest rate constant has an energy defect of 1280 cm^{-1}, and a ΔJ change of 8 is needed to obtain near-energy resonance at 300 K. The HBr reaction does follow a near-energy resonant pathway and gives HBr(2) as the main product; however, k^b_{HBr} is only ~ 5 times larger than k^b_{HCl}, which has an energy defect of 2360 cm^{-1}. Although not conclusive, the balance of the evidence is against an energy resonance pathway for HCN quenching; the HCN(001) product seems more important than HCN(011) or HCN(021). The situation

is less clear for quenching by CO_2. Emission was observed only from $CO_2(001)$; however, some of the energy resonant states, CO_2(201, 041, 121 and 002) could have been formed and rapidly deactivated. The $CO_2(002)$ level is a prime suspect as an important product channel. Mullar and Houston (Ref. 16) also observed $CO_2(001)$ emission in a time resolved study; but, the initial CO_2 vibrational distribution was not ascertained. Although Thrush and Thomas (Ref. 10) observed emission from $CO_2(021)$ and $CO_2(101)$, it is difficult to deduce initial distributions from their work. It does seem clear that CO_2 does quench $O_2(b)$ by an E-V mechanism and that this reaction is a prime case for further state-to-state studies. Such work should be feasible for high resolution experiments in which atmospheric CO_2 absorption was completely removed, since all of these levels could be monitored via the $\Delta v_3=1$ transitions. Attempts were made to observe product IR emission from quenching of $O_2(b)$ by COS, H_2S and NH_3; however, the small Einstein coefficients for the transitions with the range of our InSb detector prevented the detection of significant IR emission signals.

In the present apparatus, only the quenching of $O_2(a)$ by HF could be observed at the state-to-state level. Attempts to observe the reaction of $O_2(a)$ with HCl by adding CO_2 to the prereactor to reduce $[O_2(b)]$ gave no obvious emission that could be attributed to the $O_2(a)$ reaction. The quenching of $O_2(a)$ by HF does appear to proceed by an E-V mechanism. The data, which are not completely free of vibrational relaxation, suggest that both HF(1) and HF(2) are products. Future work to identify product states from E-V transfer, for molecules other than HF, will require one to two orders of magnitude of increased sensitivity for observation of IR emission, so that the reagent concentrations can be reduced to avoid the problem of rapid vibrational relaxation by the parent reagent. An alternative approach would be to increase the $O_2(a)$ concentration with suppression of both the $O_2(b)$ and H_2O concentrations by use of chemical generation

of $O_2(a)$. However, the very small $O_2(a)$ quenching rate constants by most simple molecules make state-to-state studies intrinsically difficult.

In addition to the state-to-state quenching studies with halogen halides, quenching rate constants for $O_2(a)$ and $O_2(b)$ by numerous other small molecules were measured. The quenching rate constants for $O_2(a)$ by CF_3NO is unusually large and an E-E mechanism is suspected.

REFERENCES

1. McDermott, W. E., Pchelkin, M. R., Bernard, D. J. and Bousels, R. R., App. Phys. Lett. 32, 469 (1978) 34, 40 (1979).

2. a. Hays, G. N. and Fisk G. A., IEEE J. Quant. Elec. QE-17, 1823 (1981).
   b. Busch, G. E., IEEE J. Quant. Elect. QE-17, 1128 (1981).
   c. Heidner, R. F. III, Gardner, C. F., Segal, G. I. and El-Sayed, T. M., J. Phys. Chem. 87, 2348 (1983).
   d. Hall, G. E., Marine, W. J. III, and Houston, P. L., J. Phys Chem. 87, 2153 (1983).
   e. Fisk, G. A. and Hays, G. N., J. Chem. Phys. 77, 4965 (1982).

3. Agrawalla, B. S., Manocha, A. S. and Setser, D. W., J. Phys. Chem. 85, 2873 (1981).

4. Bachar, J. and Rosenwaks, S., Appl. Phys. Lett. 41, 16 (1982).

5. Bachar, J. and Rosenwaks, S., Chem. Phys. Lett. 96, 526 (1983).

6. Wickramaaratchi, M. A. and Setser, D. W., J. Phys. Chem. 87, 64 (1983).

7. Wayne, R. P., Adv. Photochem, 7, 13 (1969).

8. O'Brien, R. J. Jr and Myers, G. H., J. Chem. Phys. 53, 3832 (1970).

9. a. Becker, K. H., Groth, W. and Schurath, V., Chem. Phys. Lett. 8, 259 (1971).
   b. Leiss, A., Schurath, V. Becker, K. H. and Fink, E. H., J. Photochem. 8, 211 (1978).

10. a. Thomas, R. G. O. and Thrush, B. A., Proc. Roy. Soc. A356, 287 (1977).
    b. Thomas, R. G. O. and Thrush, B. A., Proc. Roy. Soc. A356, 295 (1977).
    c. Thomas, R. G. O. and Thrush, B. A., Proc. Roy. Soc. A356, 307 (1977)
    d. Ogryzlo, E. A., and Thrush, B. A., Chem. Phys. Lett. 24, 319 (1974).

11. Madronich, S., Wiesenfeld, J. R. and Wolga, G. J., Chem. Phys. Lett. 46, 267 (1977).

12. a. Borrell, P. M., Borrell, P., Grant, K. R. and Pedley, M. D., J. Phys. Chem. 86, 700 (1982).
    b. Borrell, P. M., Borrell, P. and Grant, K. R., J. Chem. Phys. 78, 748 (1983).
    c. Boodaghians, R. B., Borrell, P. M. and Borrell, P., J. Chem. Soc. Faraday 2 19, 907 (1983).
    d. Boodaghians, R. B., Borrell, P. M. and Borrell, P., Chem. Phys. Lett. 97, 193 (1983).

13. McLarsen, I. A., Morris, N. W. and Wayne, R. P., J. Photochem. 16, 311 (1981).

14. Lawton, S. A., Novick, S. E., Broida, H. P. and Phelps. A. V., J. Chem. Phys. 66, 7381 (1977).

15. Aviles, R. G., Mullar, D. F. and Houston, P. L., Appl. Phys. Lett. 37, 358 (1980).

16. Mullar, D. F. and Houston, P. L., J. Phys. Chem. 85, 3563 (1981)

17. Kohse-hoinghaus, K. and Stuhl, F., J. Chem. Phys. 72, 3720 (1980).

18. Braithwaithe, M., Ograyzlo, E. A., Davidson, J. A. and Schiff, H. I., Chem. Phys. Lett. 42, 158 (1976).

19. a. Ogryzlo, E. A., Singlet Oxygen, ed. Wasserman, H. H. and Murray, R. W., Academic Press, New York (1979).

    b. Ogryzlo E. A., in Singlet Oxygen Reactions with Organic Compounds and Polymers, Ranby, R. and Rabek, J. F., John Wiley & Sons, New York, (1978).

20. Westenberg, A. A., Moore, J. M. and Dehass, N., Chem. Phys. Lett. 7, 597 (1970).

21. Schmidt, C. and Schiff, H. I., Chem. Phys. Lett. 23, 339 (1973).

22. Cupitt, L. T., Takacs, G. A. and Glass, G. P., Int. J. Chem. Kinet., 14, 487 (1982).

23. Winter, R., Barnes, I., Fink, E. H., Wildt, J. and Zabel, F., Chem. Phys. Lett. 73, 297 (1980).

24. McDermott, W. E. and Bernard, D. J., Chem. Phys. Lett. 64, 60 (1979).

25. Kear, K. and Abrahamson, F. W., J. Photochem. 3, 409 (1974/75).

26. Braithwaite, M., Davidson, J. A., and Ogryzlo, E. A., J. Chem. Phys. 65, 771 (1976).

27. Davidson, J. A. and Ogryzolo, E. A., Chemiluminescence and Bioluminescence (Plenum Press, New York, 1973).

28. Gauthier, M. J. E. and Snelling, D. R., J. Photochem. 4, 27 (1975).

29. a. Dzelzkalns, L. S. and Kaufman, F., J. Chem. Phys. 79, 3363 (1983).

    b. Dzelzkalns, L. S. and Kaufman, F., J. Chem. Phys. 79, 3836 (1983).

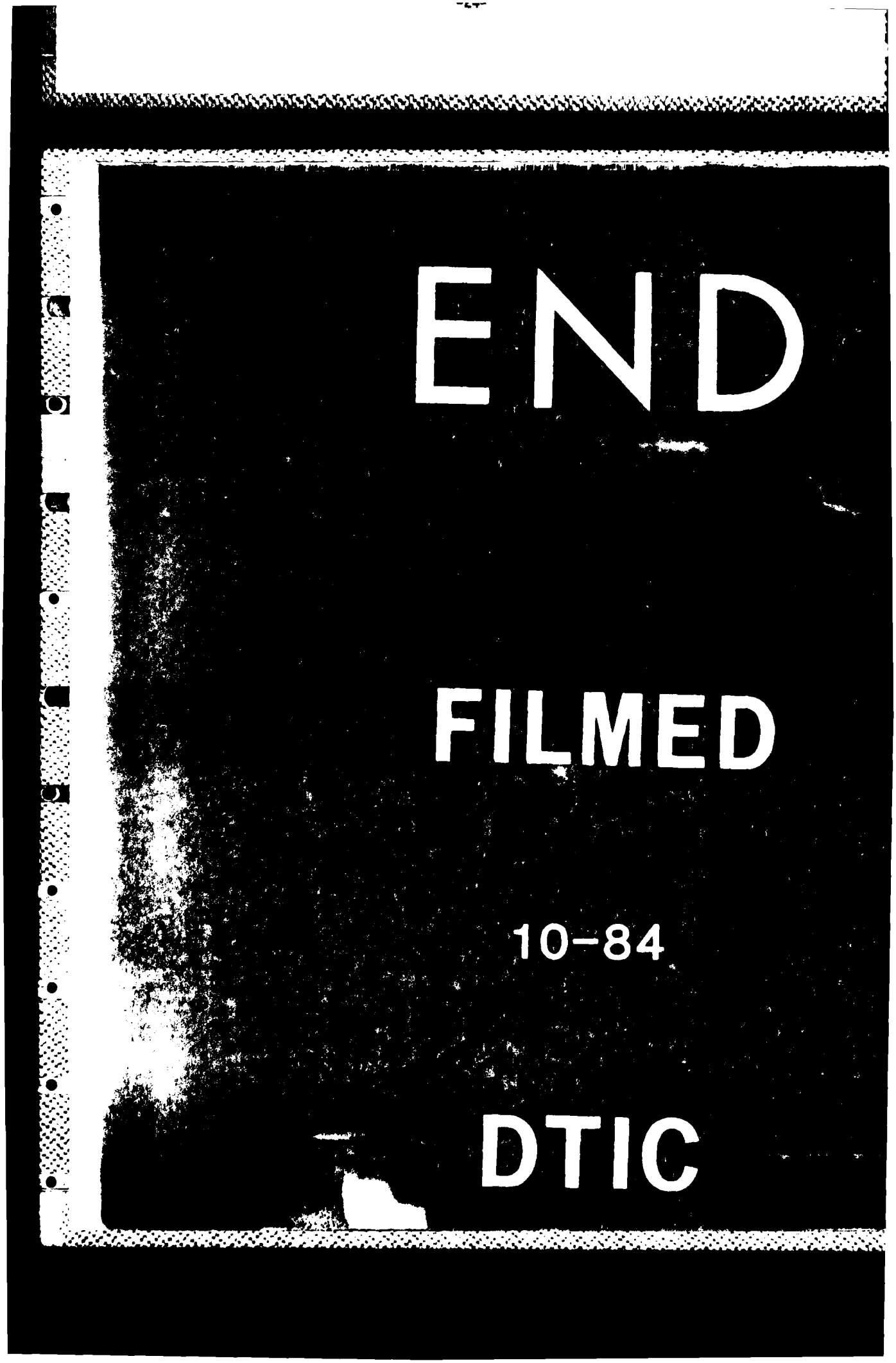
END
FILMED
10-84
DTIC